J|A|C|S ARTICLES

Published on Web 06/16/2009

Structure of Triplet Propynylidene (HCCCH) as Probed by IR, UV/vis, and EPR Spectroscopy of Isotopomers

Randal A. Seburg,[†,‡] Eric V. Patterson,[§] and Robert J. McMahon*[,†]

Department of Chemistry, University of Wisconsin, 1101 University Avenue, Madison, Wisconsin 53706, and Department of Chemistry, Truman State University, Kirksville, Missouri 63501

Received March 3, 2009; E-mail: mcmahon@chem.wisc.edu

Abstract: Spectroscopic data for triplet isotopomers H−C−C−C−H, H−^{13}C−C−C−H, and H−C−^{13}C−C−H are consistent with computational predictions for a symmetric structure in which the terminal carbons are equivalent (C_2 or C_{2v}) and are inconsistent with a planar (C_s) structure in which they are not. Experimentally observed ^{13}C isotope shifts in the IR spectra and ^{13}C hyperfine coupling constants in the EPR spectra exhibit good agreement with values predicted by theory for a C_2 structure. The ^{13}C hyperfine coupling constants also provide an independent experimental estimate for the bond angles in the molecule. The isotope-dependence of the zero-field splitting parameters reveals the influence of molecular motion in modulating the values of these parameters. The interpretation of motional effects provides a basis for rationalizing the anomalously low E value, which had previously been interpreted in terms of an axially symmetric ($D_{\infty h}$) structure. Computational studies involving Natural Bond Orbital and Natural Resonance Theory analyses provide insight into the spin densities and the complex electronic structure of this reactive intermediate.

Introduction

Triplet propynylidene (propargylene, HCCCH) represents a prototypical functionality in organic chemistry—the simplest acetylenic carbene—as well as an important chemical intermediate in the reaction of atomic carbon with hydrocarbons,[1,2] the combustion of fuel-rich hydrocarbon flames,[3,4] and the chemistry of interstellar space.[5−7] Substituted propynylidene derivatives also find use as ligands in organometallic chemistry,[8,9] where these complexes exhibit interesting reactivity that has been exploited in organic synthesis.[10,11] The structure and reactivity of HCCCH have attracted attention and controversy for decades. Three different structures—linear $D_{\infty h}$ (**1**), twisted C_2 (**2**), and bent C_s (**3**) (Scheme 1)—have been proposed on the basis of solution reactivity studies, matrix EPR and IR spectroscopy, and theoretical calculations. Paradoxically, the structure of triplet HCCCH appears to be best depicted as a nonplanar, allenic 1,3-diradical (**2**), while the reactivity reflects that of an acetylenic carbene (**1** or **3**).[12−15]

Scheme 1

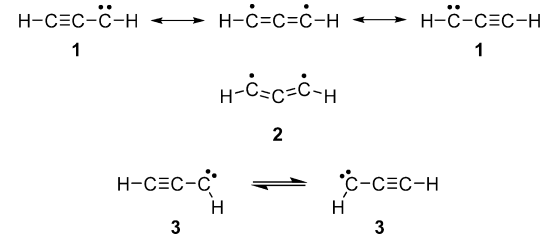

Our earlier investigations provided experimental and computational evidence in favor of a bent 1,3-allenic diradical (C_2) structure for propynylidene[16,17] and revealed the existence of isotope label-scrambling processes within the manifold of C_3H_2 isomers under photochemical conditions.[17,18] In the current investigation, we explore the electronic structure of propynylidene through a detailed analysis of IR, UV/vis, and EPR spectra of ^{13}C- and ^{2}H-labeled isotopomers (Scheme 2). The

† University of Wisconsin.
‡ Current Address: CIMA Labs, Inc., 7325 Aspen Lane, Brooklyn Park, MN 55428.
§ Truman State University.

(1) Gu, X.; Guo, Y.; Zhang, F.; Kaiser, R. I. *J. Phys. Chem. A* **2007**, *111*, 2980–2992.
(2) Leonori, F.; Petrucci, R.; Segoloni, E.; Bergeat, A.; Hickson, K. M.; Balucani, N.; Casavecchia, P. *J. Phys. Chem. A* **2008**, *112*, 1363–1379.
(3) Boullart, W.; Devriendt, K.; Borms, R.; Peeters, J. *J. Phys. Chem.* **1996**, *100*, 998–1007.
(4) Taatjes, C. A.; Klippenstein, S. J.; Hansen, N.; Miller, J. A.; Cool, T. A.; Wang, J.; Law, M. E.; Westmoreland, P. R. *Phys. Chem. Chem. Phys.* **2005**, *7*, 806–813.
(5) Kaiser, R. I. *Chem. Rev.* **2002**, *102*, 1309–1358.
(6) Herbst, E. *Chem. Soc. Rev.* **2001**, *30*, 168–176.
(7) Thaddeus, P.; McCarthy, M. C.; Travers, M. J.; Gottlieb, C. A.; Chen, W. *Faraday Discuss.* **1998**, *109*, 121–135.
(8) Casey, C. P.; Kraft, S.; Powell, D. R. *J. Am. Chem. Soc.* **2000**, *122*, 3771–3772.
(9) Casey, C. P.; Kraft, S.; Powell, D. R. *J. Am. Chem. Soc.* **2002**, *124*, 2584–2594.
(10) Padwa, A.; Austin, D. J.; Gareau, Y.; Kassir, J. M.; Xu, S. L. *J. Am. Chem. Soc.* **1993**, *115*, 2637–2647.
(11) Hansen, E. C.; Lee, D. *Acc. Chem. Res.* **2006**, *39*, 509–519.
(12) Regitz, M. In *Methoden der Organischen Chemie (Houben-Weyl)*; Thieme Verlag, G.: Stuttgart, 1989; Vol. E19b.
(13) *Carbenes*; Jones, M., Moss, R. A., Eds.; R. E. Krieger: Malabar, FL, 1983; Vol. I.
(14) *Carbenes*; Moss, R. A., Jones, M., Eds.; R. E. Krieger: Malabar, FL, 1983; Vol. II.
(15) Kirmse, W. *Carbene Chemistry*, 2nd ed.; Academic Press: New York, 1971.
(16) Seburg, R. A.; DePinto, J. T.; Patterson, E. V.; McMahon, R. J. *J. Am. Chem. Soc.* **1995**, *117*, 835–836.

10.1021/ja901606a CCC: $40.75

Scheme 2

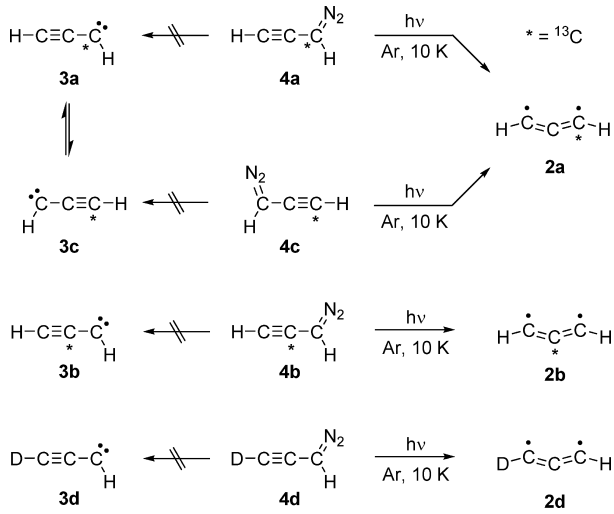

EPR spectra provide insight into both the electronic structure and the effects of molecular motion on the measured zero-field splitting parameters. The new interpretation of motional effects provides a basis for rationalizing the apparent discrepancy between earlier EPR data, which had been interpreted in terms of the $D_{\infty h}$ structure (**1**), and more recent spectroscopic and isotope labeling data, which favor the C_2 structure (**2**).

Background

Generation of propynylidene in solution in the presence of *cis*- or *trans*-2-butene resulted in partial loss of stereochemistry in the cyclopropane products, establishing the triplet state reactivity of propynylidene.[19] The gas-phase trapping by styrene of ^{14}C-labeled propynylidene, produced from the photolysis of diazopropyne-1-^{14}C (**4e**), resulted in a 1:1 ratio of labeled ethynylphenylcyclopropanes (**5**, Scheme 3), revealing equal reactivity at both terminal carbons of propynylidene.[13,14,20] Similar results were obtained when diazopropyne-3-^{3}H was photolyzed in solution with *cis*- or *trans*-2-butene.[21,22] These results were interpreted in terms of an axially symmetric structure (**1**, $D_{\infty h}$) having three *sp*-hybridized carbons.[13−15,19] Soon thereafter, the first spectroscopic observation of triplet propynylidene was reported. The small value of the zero-field splitting parameter, $E \approx 0$, from the EPR spectrum was interpreted in terms of an axially symmetric ($D_{\infty h}$) structure, **1**.[23] The IR spectrum of matrix-isolated propynylidene exhibited only one C−H stretch, which was also interpreted as evidence for **1**.[24]

The early spectroscopic data favoring structure **1** ($D_{\infty h}$) notwithstanding, theoretical studies fail to provide support for **1**. Calculations that treat electron correlation via finite-order perturbation theory predict a planar (C_s) structure **3**, essentially a "localized" triplet carbene structure.[25−28] These methods do not, however, reproduce the experimental IR spectrum,[17,24,27−31] even after applying an anharmonic treatment to two low-frequency vibrational modes.[27,28] Higher-level calculations, including those from a number of recent studies, predict a nonplanar (C_2) structure **2**.[17,32−38] Several of these studies place the C_{2v} structure higher in energy than the C_2 structure by only ca. 0.2 kcal/mol, with the C_{2v} structure as either a minimum on the potential energy surface or a transition state connecting the enantiomeric C_2 structures. The higher-level calculations do a better job of reproducing the experimental IR spectrum, although the prediction of both the position and intensity of the low-frequency vibration remains problematic.[17,32]

Scheme 3

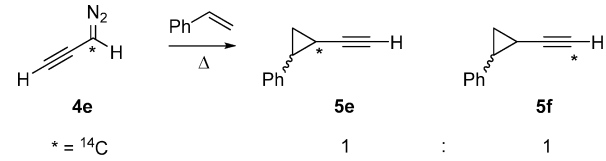

Although experiment and theory appear to be in moderately good accord concerning the IR spectrum of triplet propynylidene, aspects of EPR data and chemical reactivity are not straightforwardly reconciled in terms of a 1,3-allenic diradical structure (**2**). The large value of the zero-field splitting parameter, $D \approx 0.64$ cm^{-1}, appears to be more readily interpreted in terms of a localized carbene structure (**3**) than a 1,3-diradical structure (**2**).[15,39] EPR spectra obtained upon photolysis of 1-diazo-1,5-diphenylpentadiyne (**6**) have been ascribed to bond-shift isomers of the localized carbenes **7** and **8**,[40] while EPR spectra obtained upon photolysis of 1-phenyl- (**9**) and 3-phenyldiazopropyne (**10**) were interpreted in terms of bond-shift isomers of the localized carbenes **11** and **12** (Scheme 4).[41] It is very difficult, however, to disentangle the conformational influence of substituents, as well as conformational constraints imposed by the frozen matrix, in interpreting these EPR data. These issues have been considered, in detail, for 1,3-diphenylpropynylidene (**13**).[42,43] In terms of chemical

(17) Seburg, R. A.; Patterson, E. V.; Stanton, J. F.; McMahon, R. J. *J. Am. Chem. Soc.* **1997**, *119*, 5847–5856.
(18) Seburg, R. A.; McMahon, R. J. *Angew. Chem., Int. Ed. Engl.* **1995**, *34*, 2009–2012.
(19) Skell, P. S.; Klebe, J. *J. Am. Chem. Soc.* **1960**, *82*, 247–248.
(20) Gramas, J. V. Ph.D. Dissertation, Pennsylvania State University, 1965.
(21) Skell, P. S.; Klebe, J. In *Abstracts of Papers, 141st National Meeting of the American Chemical Society*; American Chemical Society: Washington, DC, 1962.
(22) Closs, G. L. *Top. Stereochem.* **1968**, *3*, 193–235.
(23) Bernheim, R. A.; Kempf, R. J.; Gramas, J. V.; Skell, P. S. *J. Chem. Phys.* **1965**, *43*, 196–200.
(24) Chi, F. K. Ph.D. Dissertation, Michigan State University, 1972.
(25) DeFrees, D. J.; McLean, A. D. *Astrophys. J.* **1986**, *308*, L31−L35.
(26) Jonas, V.; Böhme, M.; Frenking, G. *J. Phys. Chem.* **1992**, *96*, 1640–1648.
(27) Maier, G.; Reisenauer, H. P.; Schwab, W.; Cársky, P.; Špirko, V.; Hess, B. A.; Schaad, L. J. *J. Chem. Phys.* **1989**, *91*, 4763–4773.
(28) Cársky, P.; Špirko, V.; Hess, B. A.; Schaad, L. J. *J. Phys. Chem.* **1990**, *94*, 5493–5496.
(29) Reisenauer, H. P.; Maier, G.; Riemann, A.; Hoffmann, R. W. *Angew. Chem., Int. Ed. Engl.* **1984**, *23*, 641.
(30) Maier, G.; Reisenauer, H. P.; Schwab, W.; Cársky, P.; Hess, B. A.; Schaad, L. J. *J. Am. Chem. Soc.* **1987**, *109*, 5183–5188.
(31) Huang, J. W.; Graham, W. R. M. *J. Chem. Phys.* **1990**, *93*, 1583–1596.
(32) Herges, R.; Mebel, A. *J. Am. Chem. Soc.* **1994**, *116*, 8229–8237.
(33) Walch, S. P. *J. Chem. Phys.* **1995**, *103*, 7064–7071.
(34) Ochsenfeld, C.; Kaiser, R. I.; Lee, Y. T.; Suits, A. G.; Head-Gordon, M. *J. Chem. Phys.* **1997**, *106*, 4141–4151.
(35) Rubio, M.; Stålring, J.; Bernhardsson, A.; Lindh, R.; Roos, B. O. *Theor. Chem. Acc.* **2000**, *105*, 15–30.
(36) Ionescu, E.; Reid, S. A. *THEOCHEM* **2005**, *725*, 45–53.
(37) Mohajeri, A.; Jenabi, M. J. *THEOCHEM* **2007**, *820*, 65–73.
(38) Aguilera-Iparraguirre, J.; Boese, A. D.; Klopper, W.; Ruscic, B. *Chem. Phys.* **2008**, *346*, 56–68.
(39) Sander, W.; Bucher, G.; Wierlacher, S. *Chem. Rev.* **1993**, *93*, 1583–1621.
(40) Noro, M.; Koga, N.; Iwamura, H. *J. Am. Chem. Soc.* **1993**, *115*, 4916.
(41) Noro, M.; Masuda, T.; Ichimura, A. S.; Koga, N.; Iwamura, H. *J. Am. Chem. Soc.* **1994**, *116*, 6179–6190.
(42) DePinto, J. T.; McMahon, R. J. *J. Am. Chem. Soc.* **1993**, *115*, 12573–12574.

Scheme 4

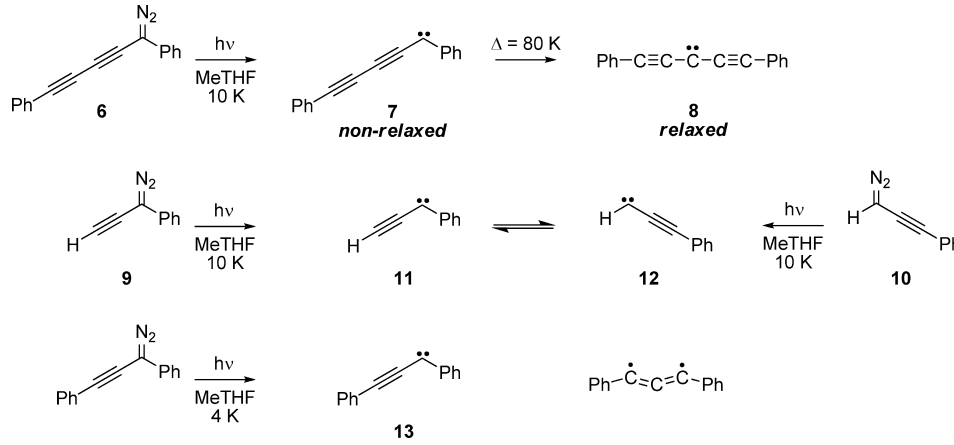

Scheme 5

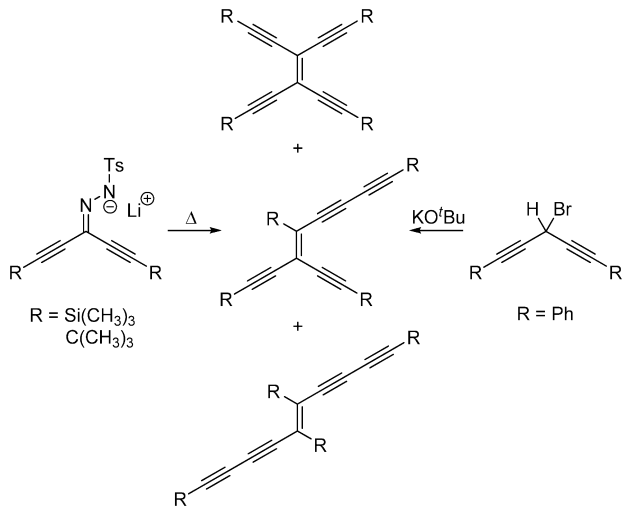

reactivity, trapping and/or dimerization products are readily reconciled in terms of carbenic reactivity. Substituted propynylidenes[44,45] and pentadiynylidenes[46,47] exhibit reactivity at multiple sites, generally interpreted as arising from bond-shift isomers of the putative acetylenic carbenes (Scheme 5).

Results

Photolysis of Diazopropyne (4). Long-wavelength irradiation ($\lambda > 472$ nm) of diazopropyne (**4**) matrix-isolated in argon at cryogenic temperatures produces triplet propynylidene (**2**: IR (Ar, 8 K) 3265 s, 1621 w, 550 m, 403 m, 249 s, 246 m cm^{-1}; UV (Ar, 8 K) λ_{max} 235, 240, 247, 252, 260, ca. 270−350 (broad absorption exhibiting vibronic fine structure) nm; EPR (Ar, 14 K) (after annealing at 37 K) $|D/hc| = 0.6401$ cm^{-1}, $|E/hc| = 0.000\,965$ cm^{-1}; Z_1 3446, X_2 5877, Y_2 5921, Z_2 10 239 G, microwave frequency = 9.5318 GHz). The difference IR spectrum depicting the disappearance of **4** and appearance of **2** is shown in Figure 1c. The IR bands of **2** agree well with those previously reported.[17,27−31] Our experiments enabled us to obtain the UV spectrum of triplet propynylidene (**2**) (Figures S3 and S4).[17]

The EPR spectrum of **2** exhibits four transitions characteristic of a randomly oriented triplet carbene (Figure 2).[67,68,85] Two distinct matrix sites are readily apparent in the X_2 transition immediately after photolysis (they are not detectable in the Y_2, Z_1, and Z_2 transitions). Annealing the matrix at 37 K results in a decrease (but not complete disappearance) of the minor site, which is still visible in Figure 2a. Although the X_2 and Y_2 transitions overlap somewhat, they are distinguishable. The magnetic field value of the X_2 line was assigned as the point at which the signal's intensity is zero. This value was estimated by interpolating between the intensity maximum and minimum of the transition. Just to the low magnetic field side of the Z_1 line is a signal due to radical impurities ($g = 2$) that appears in all of our spectra, even before any irradiation has been performed. Thus, the low-field side of the Z_1 transitions may be truncated to a small extent in our spectra.

Diazopropyne (**4**) was photolyzed ($\lambda > 472$ nm) in a nitrogen matrix to investigate further the possibility of two sites in the EPR spectrum of **2** (EPR (N_2, 14 K); site 1 (minor): $|D/hc| = 0.6465$ cm^{-1}, $|E/hc| = 0.001\,03$ cm^{-1}, Z_1 3520, X_2 5884, Y_2 5930, Z_2 10 297 G, microwave frequency = 9.5131 GHz; site 2 (major): $|D/hc| = 0.6530$ cm^{-1}, $|E/hc| = 0.001\,14$ cm^{-1}, Z_1 3589, X_2 5897, Y_2 5948, Z_2 10 369 G, microwave frequency = 9.5131 GHz). The spectrum in N_2 indeed exhibits fine structure, which we attribute to two different matrix environments for **2** (Figure 3a; see also Supporting Information). After annealing, site 1 becomes the major component and site 2 becomes the minor component. Photolysis of diazopropyne (**4**) in a methane matrix also produces **2** (EPR (CH_4, 14 K) $|D/hc| = 0.6436$ cm^{-1}, $|E/hc| = 0.000\,925$ cm^{-1}, Z_1 3483, X_2 5886, Y_2 5927, Z_2 10 276 G, microwave frequency = 9.5327 GHz). A second site was evident, but the resolution of the spectrum in CH_4 was poorer than the spectrum in argon. Annealing resulted in a decrease in the minor site. Perhaps most significant is the close similarity of the D values of **2** in the three matrices. The zero-field splitting parameters D and E of **2** and its isotopomers in various matrices are presented in Table 1.

Photolysis of Diazopropyne-1-^{13}C (4a). Long-wavelength irradiation ($\lambda > 472$ nm) of diazopropyne-1-^{13}C (**4a**) matrix-isolated in argon affords triplet propynylidene-1-^{13}C (**2a**: IR (Ar, 8 K) 3273 w, 3257 m, 1612 w, 547 m, 402 m, 247 s, 245 sh cm^{-1}; UV (Ar, 8 K) 231, 234, 240, 246, 251, 260, 275−350

(43) DePinto, J. T.; deProphetis, W. A.; Menke, J. L.; McMahon, R. J. *J. Am. Chem. Soc.* **2007**, *129*, 2308–2315.
(44) Franck-Neumann, M.; Geoffroy, P.; Lohmann, J. J. *Tetrahedron Lett.* **1983**, *24*, 1775–1778.
(45) Franck-Neumann, M.; Geoffroy, P. *Tetrahedron Lett.* **1983**, *24*, 1779–1782.
(46) Hauptmann, H. *Tetrahedron* **1976**, *32*, 1293–1297.
(47) Hori, Y.; Noda, K.; Kobayashi, S.; Taniguchi, H. *Tetrahedron Lett.* **1969**, 3563–3566.

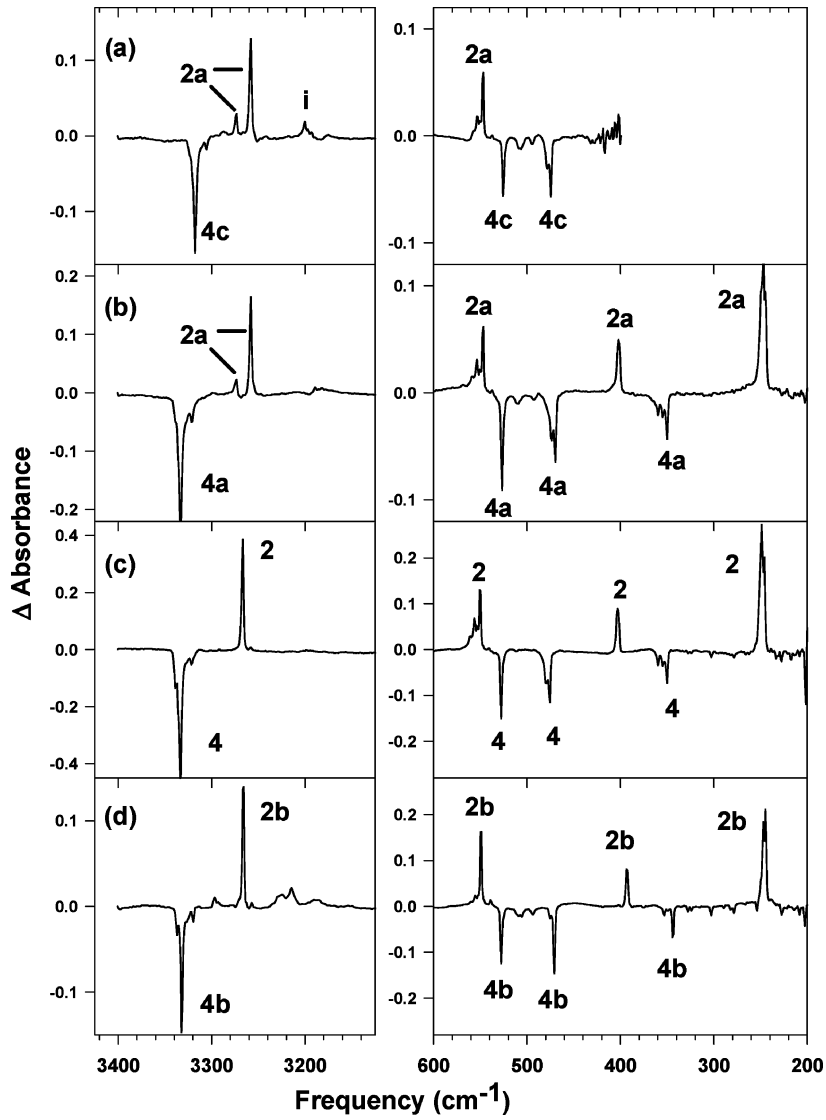

Figure 1. IR difference spectra (Ar, 8 K): (a) Disappearance of diazopropyne-3-^{13}C (**4c**) and appearance of propynylidene-1-^{13}C (**2a**) upon photolysis ($\lambda >$ 472 nm) of **4c**. The peak marked **i** does not behave as the propynylidene-1-^{13}C peaks upon further photolyses and is thus assigned as an impurity. (b) Disappearance of diazopropyne-1-^{13}C (**4a**) and appearance of propynylidene-1-^{13}C (**2a**) upon photolysis ($\lambda >$ 472 nm) of **4a**. (c) Disappearance of diazopropyne (**4**) and appearance of propynylidene (**2**) upon photolysis ($\lambda >$ 472 nm) of **4**. (d) Disappearance of diazopropyne-2-^{13}C (**4b**) and appearance of propynylidene-2-^{13}C (**2b**) upon photolysis ($\lambda >$ 472 nm) of **4b**.

(broad absorption exhibiting vibronic structure) nm; EPR (Ar, 14 K) $|D/hc| = 0.6412$ cm^{-1}, $|E/hc| = 0.001\,08$ cm^{-1}; Z_1 3453, X_2 5873, Y_2 5922, Z_2 10 243 G, microwave frequency = 9.5324 GHz; $A_X = A_Y = 38$ G, $A_Z = 7.4$ G). The matrices of **2a** do not contain a detectable quantity of the isotopomer **2b**, as judged by IR spectroscopy. The difference IR spectrum depicting the disappearance of **4a** and the appearance of **2a** is shown in Figure 1b. The C−H stretching region is of greatest importance. Two bands are present for **2a**, a weak band at 3273 cm^{-1} and a stronger one at 3257 cm^{-1}, where only one existed for unlabeled **2** at 3265 cm^{-1}. The C−C−C stretching mode of **2a** (1612 cm^{-1}) exhibits a shift of 9 cm^{-1} to lower frequency, relative to **2**. The other bands differ only slightly from those of **2**. The UV spectrum of **2a** is not appreciably different than that of **2**.

The EPR spectrum of propynylidene-1-^{13}C (**2a**) obtained upon irradiation ($\lambda >$ 472 nm) of diazopropyne-1-^{13}C (**4a**) in argon is displayed in Figure 2b. Comparison of this spectrum with that of unlabeled **2** reveals significant ^{13}C-hyperfine splitting (hfs) in the X_2 and Y_2 transitions of **2a**. The ^{13}C-hyperfine constants of **2a** are presented in Table 2. To determine the hfs constants A_X and A_Y—the components of the hyperfine interaction in the direction of the *x*- and *y*-molecular axes (perpendicular to the quasi long axis of the molecule)—we simulated the EPR spectra that would result upon introduction of hyperfine couplings of varying magnitude into the spectrum of unlabeled propynylidene (**2**). The details of this simulation procedure are explained in the Supporting Information. Figure 4 shows the experimental and simulated EPR spectra of **2a** for the X_2/Y_2 transitions. An extremely good reproduction of the experimental spectrum is obtained using $A_X = A_Y = 38$ G, and thus we assign this value to the *x*- and *y*-components of the ^{13}C-hyperfine interaction in **2a**. The magnitude of the hyperfine interaction in the Z_1 and Z_2 lines is much smaller, seen only as a broadening of the signals (Figure 2). The hfs constant A_Z was determined by measuring the full width at half-maximum (fwhm) of the Z_2 transition of **2a** and subtracting the corresponding fwhm of the Z_2 transition of unlabeled **2** from it. A_Z cannot be obtained from

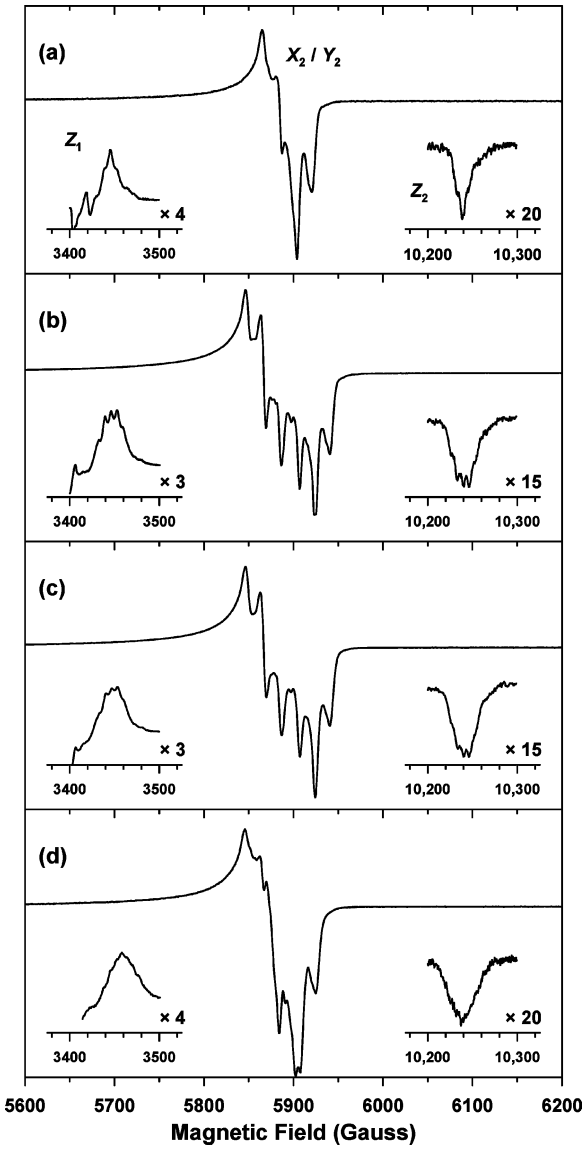

Figure 2. Triplet EPR spectra (Ar, 10 K), obtained upon irradiation ($\lambda >$ 472 nm) of the diazo compound precursor, followed by annealing at ca. 37 K. (a) Propynylidene (**2**), from diazopropyne (**4**). (b) Propynylidene-1-^{13}C (**2a**), from diazopropyne-1-^{13}C (**4a**). (c) Propynylidene-1-^{13}C (**2a**), from diazopropyne-3-^{13}C (**4c**). (d) Propynylidene-2-^{13}C (**2b**), from diazopropyne-2-^{13}C (**4b**).

the Z_1 transition because the signal due to radical impurities (g = 2) truncates the low-field side of the transition.

Measurement of the ^{13}C-hfs constants A_X, A_Y, and A_Z enables the determination of the experimental isotropic (A_I) and anisotropic (A_{an}) ^{13}C-hfs constants via the relationships

$$A_I = {}^1/_3[A_X + A_Y + A_Z]$$

$$(A_X)_{an} = A_X - A_I$$

Although the values of A_X, A_Y, and A_Z may not be diagonalized principal components of the hyperfine interaction tensor, and although the **g**, **D**, and **A** tensors may be non-collinear, the value of the isotropic component, A_I, is not affected.[49]

(48) Smith, G. R.; Weltner, W., Jr. *J. Chem. Phys.* **1975**, *62*, 4592–4604.
(49) Golding, R. M.; Tennant, W. C. *Mol. Phys.* **1973**, *25*, 1163–1171.

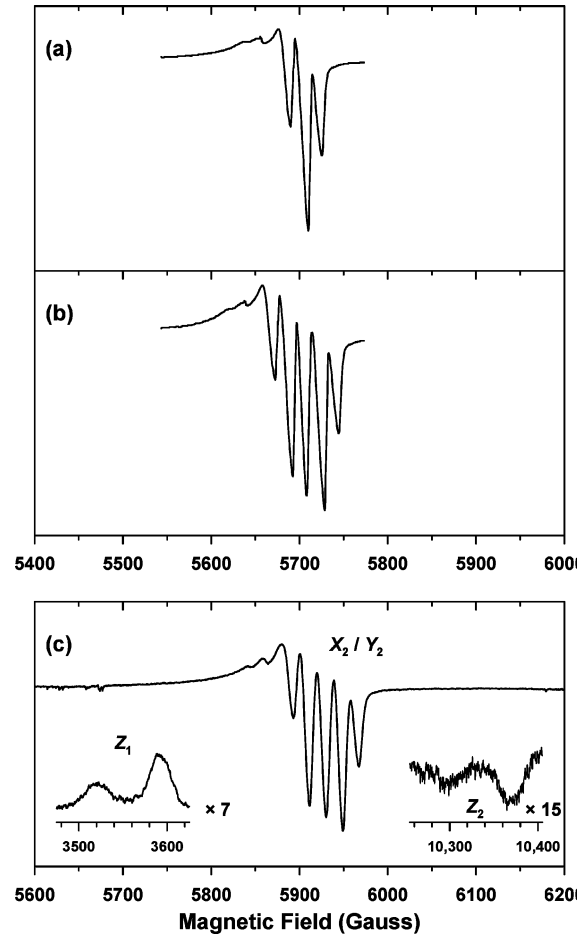

Figure 3. Triplet EPR spectra (N_2, 13 K). (a) Propynylidene (**2**), obtained upon irradiation ($\lambda >$ 472 nm) of diazopropyne (**4**). (b) Simulation of the X_2 and Y_2 transitions of propynylidene-1-^{13}C (**2a**) using ^{13}C-hyperfine splitting constant $A_X = A_Y$ = 38 G. (c) Propynylidene-1-^{13}C (**2a**), obtained upon irradiation ($\lambda >$ 472 nm) of diazopropyne-1-^{13}C (**4a**). The 200 G offset in (c) facilitates comparison with (a) and (b) and arises from the difference in microwave frequency between the two experiments.

Table 1. Zero-Field Splitting Parameters |*D*/*hc*| and |*E*/*hc*| of Triplet Propynylidene Isotopomers[a]

isotopomer	matrix	|*D*/*hc*|	|*E*/*hc*|
H−C−C−C−H (**2**)	argon	0.6401	0.000 96
	nitrogen (site 1)	0.6465	0.001 03
		0.6456[b]	
	nitrogen (site 2)	0.6530	0.001 14
		0.6521[b]	
	methane	0.6436	0.000 92
	CTFE[c]	0.6276	<0.00 08
H−^{13}C−C−C−H (**2a**)[d]	argon	0.6412	0.001 08
	nitrogen (site 1)	0.6464[b]	---[e]
	nitrogen (site 2)	0.6532[b]	---[e]
H−^{13}C−C−C−H (**2a**)[f]	argon	0.6409	0.001 06
H−C−^{13}C−C−H (**2b**)	argon	0.6406	0.001 08
^{2}H−C−C−C−H (**2d**)	argon	0.6449	0.000 87

[a] |*D*/*hc*| and |*E*/*hc*| in cm^{-1}. [b] Calculated from the Z_1 and Z_2 transitions only. [c] Poly(chlorotrifluoro ethylene), ref 23. [d] From diazopropyne-1-^{13}C (**4a**). [e] Superposition of two sites and extensive ^{13}C-hyperfine splitting in these lines preclude an accurate determination of |*E*/*hc*|. [f] From diazopropyne-3-^{13}C (**4c**).

The EPR spectrum of propynylidene-1-^{13}C (**2a**) obtained upon irradiation ($\lambda >$ 472 nm) of diazopropyne-1-^{13}C (**4a**) in nitrogen is displayed in Figure 3c. As in the case of the unlabeled isotopomer (**2**), two distinct sites in the nitrogen matrix are easily

Table 2. Experimental ^{13}C-Hyperfine Splitting Constants of Triplet Propynylidene and CCO Isotopomers[a]

hfc	H^{13}CCCH (**2a**)[b]	HC^{13}CCH (**2b**)[b]	^{13}CCO[c]	C^{13}CO[c]
A_X	38	24	20	9.3
A_Y	38	24	20	9.3
A_Z	7.1	9.3	6.1	11
A_I	28	19	16	11
$(A_X)_{an}$	10	5	4	−1.7
$(A_Z)_{an}$	−20.9	−9.7	−9.9	0

[a] Hyperfine splittings are in Gauss. [b] This work. Propynylidene (**2**) matrix-isolated in argon. [c] From ref 48. CCO matrix-isolated in neon.

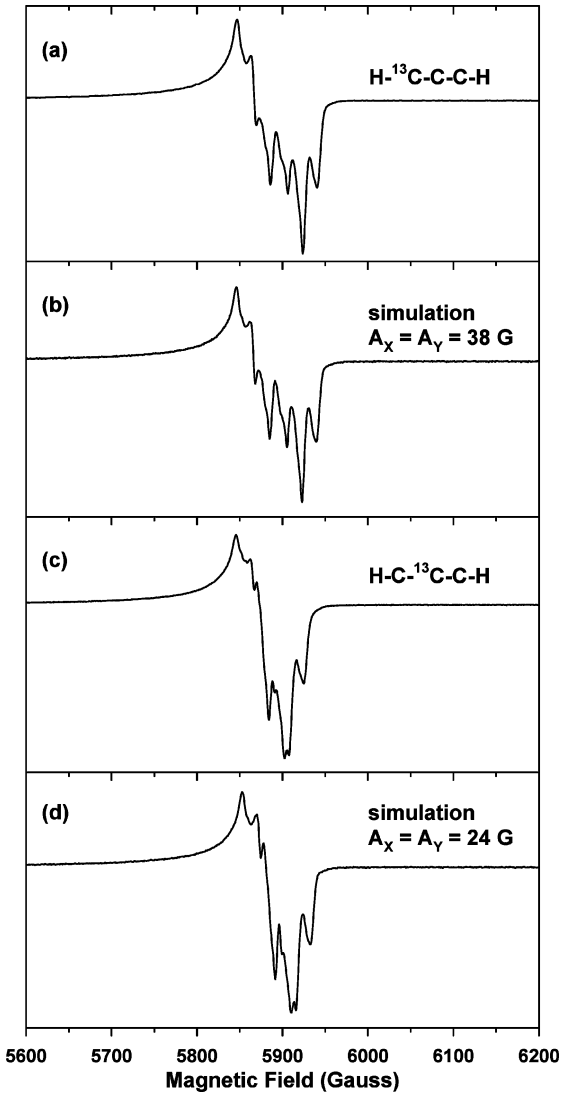

Figure 4. EPR spectra. (a) X_2 and Y_2 transitions of triplet propynylidene-1-^{13}C (**2a**) (Ar, 13 K), obtained upon irradiation (λ > 472 nm) of diazopropyne-3-^{13}C (**4c**). (b) Spectral simulation of **2a** using ^{13}C-hyperfine splitting constant $A_X = A_Y = 38$ G. (c) X_2 and Y_2 transitions of propynylidene-2-^{13}C (**2b**) (Ar, 13 K), obtained upon irradiation (λ > 472 nm) of diazopropyne-2-^{13}C (**4b**). (d) Spectral simulation of **2b** using ^{13}C-hyperfine splitting constant $A_X = A_Y = 24$ G.

distinguished in the Z_1 and Z_2 transitions (site 1: $|D/hc| = 6464$ cm^{-1}, Z_1 3521, Z_2 10 299 G; site 2: $|D/hc| = 0.6532$ cm^{-1}, Z_1 3592, Z_2 10 371 G; microwave frequency = 9.5107 GHz). The ^{13}C-hyperfine splitting is not resolvable in the Z_1 and Z_2 transitions, appearing only as a broadening of the signals; however, the X_2 and Y_2 signals clearly exhibit resolved hfs. The X_2 and Y_2 transitions are not easily interpreted by inspection,

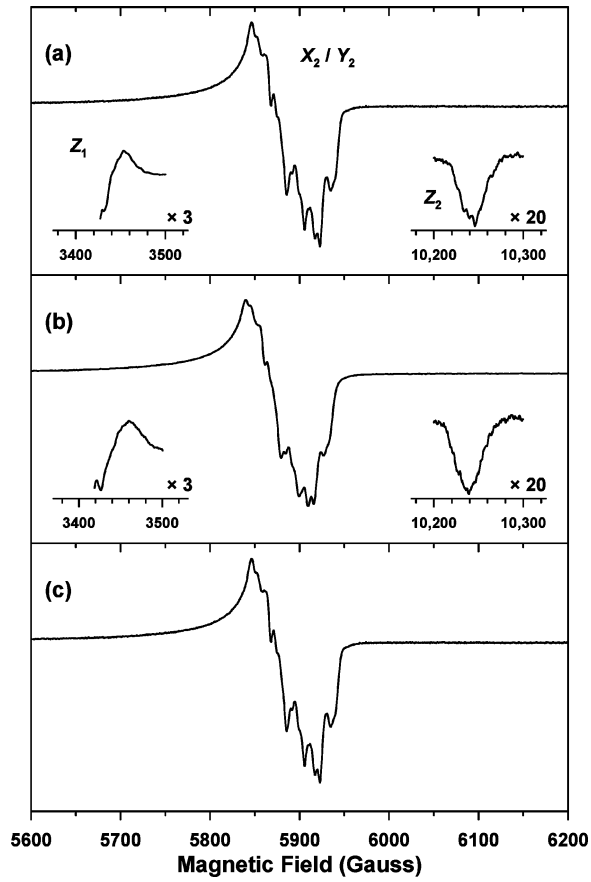

Figure 5. (a) EPR spectrum of a 2:1 mixture of propynylidene-1-^{13}C (**2a**) and propynylidene-2-^{13}C (**2b**), respectively, obtained upon irradiation (λ > 237 nm) of an Ar matrix containing only **2a**. (b) EPR spectrum of a 2:1 mixture of **2a** and **2b**, respectively, obtained upon irradiation (λ > 237 nm) of an Ar matrix containing only **2b**. (c) Spectral simulation of the X_2 and Y_2 transitions of a 2:1 mixture of triplet species having ^{13}C-hyperfine splitting constants of $A_X = A_Y = 38$ G and $A_X = A_Y = 24$ G, respectively.

the complexity arising through the combination of matrix sites and hyperfine splitting. Simulation of the X_2 and Y_2 region of the EPR spectrum of **2a** in nitrogen is not as definitive as the argon case, due to the high proportion of the second matrix site. Nevertheless, the best fits occur in the range of $A_X = A_Y = 36$ to 38 G. Figure 3b shows the simulation where $A_X = A_Y = 38$ G.

Broad-band irradiation (λ > 237 nm) of an argon matrix containing only **2a** results in the statistical scrambling of the ^{13}C label among several different C_3H_2 isomers.[17,18] Figure 5a presents the EPR spectrum after this automerization occurs, revealing the formation of the center-labeled isotopomer **2b**. The experimental spectrum in the X_2 and Y_2 region is reproduced most satisfactorily by simulating a spectrum of a 2:1 mixture of propynylidenes with ^{13}C-hyperfine splitting constants of $A_X = A_Y = 38$ G and $A_X = A_Y = 24$ G, respectively, as shown in Figure 5c. The same irradiation conditions in the corresponding IR experiments cause the IR bands of **2b** to grow (*vide infra*) at the expense of **2a**.

Photolysis of Diazopropyne-2-^{13}C (4b). Long-wavelength irradiation (λ > 472 nm) of diazopropyne-2-^{13}C (**4b**) matrix-isolated in argon produces triplet propynylidene-2-^{13}C (**2b**: IR (Ar, 8 K) 3265 m, 1581 w, 550 m, 393 m, 247 s, 245 s cm^{-1}; EPR (Ar, 14 K) $|D/hc| = 0.6406$ cm^{-1}, $|E/hc| = 0.00\,108$ cm^{-1}; Z_1 3458, X_2 5865, Y_2 5913, Z_2 10 239 G, microwave frequency = 9.5126 GHz; $A_X = A_Y = 24$ G, $A_Z = 9.3$ G). The matrices

of **2b** do not contain a detectable quantity of isotopomer **2a**, as judged by IR spectroscopy. The difference IR spectrum depicting the disappearance of **4b** and the appearance of **2b** is shown in Figure 1d. By far the greatest band shift due to the ^{13}C-isotopic substitution in **2b** is in the C−C−C stretching mode (1581 cm^{-1}), which appears 40 cm^{-1} lower in frequency, relative to unlabeled **2**. Only one other band exhibits a significant change in frequency: the 403 cm^{-1} band in **2** shifts to 393 cm^{-1} in **2b**. All other bands differ by less than 2 cm^{-1}. In accord with expectations, the symmetrically labeled isotopomer (**2b**) exhibits only one C−H stretch in the IR spectrum (3265 cm^{-1}), in contrast to the unsymmetrically labeled isotopomer (**2a**).

Figure 2d shows the EPR spectrum of propynylidene-2-^{13}C (**2b**). Significant ^{13}C-hyperfine splitting is apparent in the spectrum of **2b** upon comparison with that of unlabeled **2** (Figure 2a). The X_2 and Y_2 transitions exhibit resolved hyperfine splitting, whereas, in the Z_1 and Z_2 regions, the splitting manifests itself as an unresolved broadening of the signals. Figure 4 shows the experimental and simulated EPR spectra of **2b** for the X_2/Y_2 transitions. The simulation using $A_X = A_Y =$ 24 G best reproduces the experimental spectrum; therefore, we assign this value to the *x*- and *y*-components of the ^{13}C-hyperfine interaction in **2b**. This value agrees with the one obtained independently from the simulation of the EPR spectrum generated by photolysis ($\lambda > 237$ nm) of **2a** (*vide supra*, Figure 5). The ^{13}C-hfs constants are summarized in Table 2.

Broadband irradiation ($\lambda > 237$ nm) of an argon matrix containing only **2b** forms a 2:1 mixture of **2a** and **2b**, respectively.[17,18] Figure 5b illustrates this automerization process in the X_2 and Y_2 region of the EPR spectrum; corresponding IR spectra provide further evidence for this process. This photolysis produces the same EPR spectrum as that of the corresponding photolysis of **2a** (*vide supra*). Thus, one is able to generate the photoequilibrium mixture of **2a** and **2b** from both directions.

Photolysis of Diazopropyne-3-^{13}C (4c). Long-wavelength irradiation ($\lambda > 472$ nm) of diazopropyne-3-^{13}C (**4c**) in an argon matrix produces propynylidene-1-^{13}C (**2a**: IR (Ar, 8 K) 3273 w, 3257 m, 1612 w, 547 m, 403 m cm^{-1}; EPR (Ar, 14 K) $|D/hc| = 0.6409$ cm^{-1}, $|E/hc| = 0.001\,06$ cm^{-1}; Z_1 3454, X_2 5874, Y_2 5922, Z_2 10 246 G, microwave frequency = 9.5319 GHz; $A_X = A_Y = 38$ G, $A_Z = 6.8$ G). The matrices of **2a** do not contain a detectable quantity of isotopomer **2b**, as judged by IR spectroscopy. The difference IR spectrum depicting the disappearance of **4c** and the appearance of **2a** is shown in Figure 1a. (Upon further irradiation, the small peak near 3200 cm^{-1} does not exhibit the same behavior as the bands assigned to propynylidene **2a**. This absorption thus represents a minor, unassigned impurity in the matrix.) The EPR spectrum of **2a** obtained from the photolysis ($\lambda > 472$ nm) of diazopropyne-3-^{13}C (**4c**) is shown in Figure 2c. It is important to note that the IR and EPR spectra that result from photolysis of diazo compound **4c** are identical to those produced from **4a**. Simulation of the ^{13}C-hfs in the X_2 and Y_2 region yields $A_X = A_Y = 38$ G, as before. Broad-band irradiation ($\lambda > 237$ nm) of a matrix of **2a** resulting from initial photolysis of **4c** also induces automerization of **2a** to **2b**, as in the cases of **4a** and **4b** (*vide supra*).

Photolysis of Diazopropyne-3-^{2}H (4d). Long-wavelength irradiation ($\lambda > 472$ nm) of **4d** matrix-isolated in Ar renders propynylidene-1-^{2}H (**2d**: IR (Ar, 8 K) 3271 s, 2469 m, 1640 w, 1580 w, 550 m, 416 w cm^{-1}; EPR (Ar, 14 K) $|D/hc| = 0.6449$ cm^{-1}, $|E/hc| = 0.000\,868$ cm^{-1}; Z_1 3497, X_2 5883, Y_2 5922, Z_2 10 295 G, microwave frequency = 9.5332 GHz). The diazo compound **4d** was contaminated with ca. 25% of the diprotio (unlabeled) species **4**, and thus the IR and EPR spectra exhibit transitions due to unlabeled **2**, as well. The Z_1 and Z_2 transitions of **2d** are displaced by 45 G to higher field from the contaminant **2**, allowing accurate assignment of magnetic field values to these lines. Thus, an accurate determination of *D* is possible. Assignment of the magnetic field values of the X_2 and Y_2 lines of **2d**, however, is less certain because the corresponding lines of **2** fall at or near the same magnetic field, making the calculated *E* value less certain. The observed IR bands of **2d** (Table S2) agree with those reported by Maier et al.[27]

Table 3. Computational Data for Triplet Propynylidene and the Allyl Radical[a]

	HCCCH	HCCCH	HCCCH	allyl radical
	1 ($D_{\infty h}$)	**2** (C_2)	**3** (C_s)	C_{2v}
relative *E*	0.19	0.00	0.01	
NIMAG	4	0	1	
eel. *E* + ZPVE	−0.67	0.00	0.12	
*r*CH	1.0652	1.0673	1.0687	
*r*CC	1.2715	1.2747	1.2862	
*a*HCC	180.0	162.1	156.5	120.9/121.5
*a*CCC	180.0	174.5	174.9	124.4
*d*HCCC		−141.2		
*r*C3H2			1.0654	
*r*C2C3			1.2628	
*a*C2C3H2			176.3	
A_I (C1, C3)	18.1	25.0	31.8/16.7	16.8
A_I (C2)	−27.7	−23.8	−24.4	−19.1
A_I (C1, C3)[b]	19.3	26.6	31.8/16.7	18.5
A_I (C2)[b]	−23.2	−19.7	−24.4	−16.1

[a] QCISD/6-311+G(2df,p) optimized structures; energy (kcal/mol), bond length (angstrom), bond angle (degrees), isotropic Fermi contact coupling, A_I, (gauss). [b] B3LYP/EPR-III // QCISD/6-311+G(2df,p).

Computational Studies. The electronic structure of triplet propynylidene (**2**) was investigated by Natural Bond Orbital (NBO) and Natural Resonance Theory (NRT)[50] analyses of the QCISD/6-311+G(2df,p) wave function of **2**. The QCISD level of theory, with a suitably large basis set, has proven to afford reliable structures and energies for C_3H_2 isomers.[18,32,51] Computational data for optimized structures of triplet HC_3H isomers **1** ($D_{\infty h}$), **2** (C_2), and **3** (C_s) are summarized in Table 3. These calculations predict a C_2-symmetric structure for triplet **2**, and the geometry of **2** (Figure 6) exhibits excellent agreement with that previously obtained at the CCSD(T)/cc-pVTZ level.[17] Refined predictions for the isotropic Fermi contact couplings were obtained using the procedure of Barone (B3LYP/EPR-III).[52] Table 4 presents the valence electron population of **2** by atom, separated into α- and β-electrons since the wave function is UHF. Table 4 also presents the spin density at each carbon. Tables 5 (α-spins) and 6 (β-spins) give a more detailed look at the electron distribution in **2**, focusing on the π-bonds and the nonbonded electrons. These tables present the electron occupancy of the natural bond orbitals (NBO), the distribution or polarization of the electrons within the NBOs, and the hybrid-

(50) Glendening, E. D.; Badenhoop, J. K.; Reed, A. E.; Carpenter, J. E.; Bohmann, J. A.; Morales, C. M.; Weinhold, F. NBO 5.0; Theoretical Chemistry Institute, University of Wisconsin: Madison, WI, 2001.
(51) Patterson, E. V. Ph.D. Dissertation, University of Wisconsin, 1996.
(52) Barone, V. In *Recent Advances in Density Functional Methods (Part I)*; Chong, D. P., Ed.; World Scientific Publishing Co.: Singapore, 1996; pp 287−334.

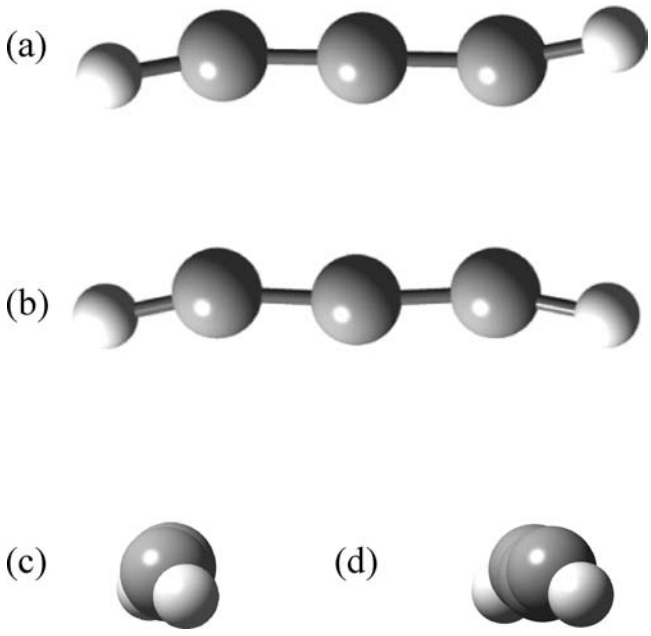

Figure 6. Computed structure for triplet propynylidene (**2**) (QCISD/6-311+G(2df,p)): (a) view down *x*-axis (C_2 axis), (b) view down *y*-axis, (c) view down *z*-axis, (d) slight rotation applied to the view in (c).

Table 4. Computed Valence Electron Population and Spin Densities for Triplet Propynylidene (**2**)[a]

atom	total population	α-electrons	β-electrons	spin density[b]
H	0.783 08	0.370 87	0.412 20	−0.041 04
C-1	4.045 20	2.634 94	1.410 25	1.241 52
C-2	4.172 11	1.885 32	2.286 79	−0.400 96
C-3	4.045 20	2.634 94	1.410 25	1.241 52
H	0.783 08	0.370 87	0.412 20	−0.041 04
total	13.828 65	7.896 95	5.931 70	2.000 00

[a] From the Natural Bond Orbital (NBO) analysis of the QCSID/6-311+G(2df,p) wave function of **2**. [b] The difference of the α- and β-populations at each atom.

ization of the constituent natural atomic orbitals (NAOs) which comprise the NBOs.

Discussion

Structure of Triplet HCCCH. An important objective of this investigation was to probe the basis for the incongruity between IR and EPR evidence concerning the structure for triplet HCCCH. In our analysis, the $D_{\infty h}$ structure (**1**) (Scheme 1) is discounted because the small E value of propynylidene is an artifact of motion in its matrix sites (*vide infra*) and because ab initio calculations do not predict a linear geometry for propynylidene. The C_2 (**2**) and C_s (**3**) structures are considered in detail. As described earlier, structure **3** is capable of exhibiting bond-shift isomerism. In unlabeled **3**, the two isomers are equivalent and thus indistinguishable. To break the degeneracy in **3** (or to differentiate the two equivalent ends of **2**), a ^{13}C-label was incorporated into the diazo compound precursors. Scheme 2 illustrates the means by which mechanistic information obtained from isotopic labeling enables one to assign a structure to triplet propynylidene. If the C_s structure is correct, the two ^{13}C-isotopomers of **3** will exhibit different IR and EPR spectra; if the C_2 structure is correct, only one IR and one EPR spectrum will be observed.

The crucial experimental result is the following: upon separate photolyses of the isotopomers diazopropyne-1-^{13}C (**4a**) and diazopropyne-3-^{13}C (**4c**), *the IR and EPR spectra are identical*, illustrated in convincing form by Figures 1 and 2. The IR bands produced upon photolysis of the two isotopomeric diazo precursors correspond in both frequency and relative intensity. The EPR spectra exhibit identical ^{13}C-hyperfine splittings. These results are consistent with the formation of one C_2 structure **2** for propynylidene. They are inconsistent with the formation of discrete C_s isotopomers (**3a** or **3c**) from each diazo compound, for in this case one would expect to observe distinguishable IR and EPR spectra. A third possibility exists, however, which is consistent with this data: formation of two C_s species (**3a** and **3c**) in an equilibrium ratio. This is a plausible hypothesis, for the energy present in the nascent propynylidene molecule upon photolysis of the diazo precursor may be dissipated too slowly

Table 5. Natural Bond Orbital Analysis of the Alpha (α)-Electrons of Triplet Propynylidene (**2**)[a]

bond	occupancy	atom	distribution of electron density (%)	hybridization of NAO[b]
H−C1 (σ)	0.98	H	36.6	s
		C-1	63.4	$sp^{1.07}$
C1−C2 (σ)	0.98	C-1	49.6	$sp^{0.94}$
		C-2	50.4	$sp^{1.01}$
C2−C3 (σ)	0.98	C-2	50.6	$sp^{1.02}$
		C-3	49.5	$sp^{0.95}$
C2−C3 (π)	0.97	C-2	26.9	$sp^{99.99}d^{0.15}f^{0.16}$
		C-3	73.1	$sp^{99.99}d^{0.05}f^{0.03}$
C2−C3 (π)	0.97	C-2	29.2	$sp^{99.99}d^{3.84}f^{4.15}$
		C-3	70.8	$sp^{99.99}d^{0.54}f^{0.28}$
C3−H (σ)	0.98	C-3	63.0	$sp^{1.10}$
		H	37.0	s
nonbonded[c]	0.77	C-1	100	$sp^{99.99}d^{0.40}f^{0.41}$
nonbonded[c]	0.75	C-1	100	$sp^{99.99}d^{0.63}f^{0.53}$
C2−C3 (π*)	0.25	C-2	73.1	$sp^{99.99}d^{0.15}f^{0.16}$
		C-3	26.9	$sp^{99.99}d^{0.05}f^{0.03}$
C2−C3 (π*)	0.22	C-2	70.8	$sp^{99.99}d^{3.84}f^{4.15}$
		C-3	29.2	$sp^{99.99}d^{0.54}f^{0.28}$
hyperbond	1.96	C1 (l.p.)	47.7	
		C2−C3 (π)	52.3	
hyperbond	1.95	C1 (l.p.)	52.8	
		C2−C3 (π)	47.2	

[a] Using the QCISD/6-311+G(2df,p) wave function of **2**. [b] Natural Atomic Orbital. [c] These are the nominal unpaired α-spins comprising the diradical character of **2**.

Table 6. Natural Bond Orbital Analysis of the Beta (β)-Electrons of Triplet Propynylidene (**2**)[a]

bond	occupancy	atom	distribution of electron density (%)	hybridization of NAO[b]
H−C1 (σ)	0.97	H	41.7	s
		C-1	58.3	$sp^{1.01}$
C1−C2 (σ)	0.98	C-1	45.5	$sp^{1.01}$
		C-2	54.5	$sp^{1.00}$
C1−C2 (π)	0.78	C-1	23.1	$sp^{99.99}d^{12.99}f^{1.14}$
		C-2	76.9	$sp^{99.99}d^{0.01}f^{0.59}$
C1−C2 (π)	0.78	C-1	22.9	$sp^{99.99}d^{0.18}f^{0.02}$
		C-2	77.1	$sp^{99.99}d^{0.02}f^{0.76}$
C2−C3 (σ)	0.98	C-2	54.5	$sp^{1.01}$
		C-3	45.5	$sp^{1.01}$
C3−H (σ)	0.98	C-3	58.3	$sp^{1.03}$
		H	41.7	s
nonbonded*	0.20	C-3	100	p
nonbonded*	0.19	C-3	100	$sp^{96.56}d^{0.11}f^{0.02}$
C1−C2 (π*)	0.02	C-1	76.9	$sp^{99.99}d^{12.99}f^{1.14}$
		C-2	23.1	$sp^{99.99}d^{0.01}f^{0.59}$
C1−C2 (π*)	0.02	C-1	77.1	$sp^{99.99}d^{0.18}f^{0.02}$
		C-2	22.9	$sp^{99.99}d^{0.02}f^{0.76}$

[a] Using the QCISD/6-311+G(2df,p) wave function of **2**. [b] Natural Atomic Orbital.

by the matrix to prevent facile bond-shift isomerization to the other isotopomer (the predicted barrier to this rearrangement is only 0.09 kcal/mol at the MP4/6-311++G(*df*,*pd*)//MP3/6-31G(*d*) level of theory[25]). Nevertheless, four lines of reasoning argue for the formation of a single species (C_2, **2a**) and against the formation of two species (C_s, **3a** and **3c**) in an equilibrium ratio.

1. The experimental IR spectra of triplet HCCCH isotopomers exhibit good agreement with the predicted IR spectra of C_2-symmetric **2** isotopomers, computed using QCISD/6-31G*[18,32] or CCSD(T)/cc-pVTZ.[17] Herges and Mebel first established that the experimental IR spectrum of unlabeled H−C−C−C−H exhibits much better agreement with the IR spectrum predicted (QCISD/6-31G*) for C_2-symmetric **2** than with the IR spectrum predicted (MP2/6-31G*) for C_s-symmetric **3**. Our results expand this observation to include the mono-^{13}C and ^{2}H isotopomers. Comparison of the experimental IR spectrum of H−^{13}C−C−C−H with (i) the computed spectrum for C_2-symmetric **2a** (CCSD(T)/cc-pVTZ) and (ii) a 1:1 mixture of C_s-symmetric isotopomers **3a** and **3c** (MP2/6-31G*) (Table S1) reveals much better agreement for C_2-symmetric **2a** with respect to harmonic vibrational frequencies, IR intensities, and isotope shifts.[17] The MP2/6-31G* calculations for the mixture of C_s structures (**3a** and **3c**) predict that two pairs of C−H stretching vibrations should be observed, with the two pairs separated by ca. 100 cm^{-1} and the bands within the pairs separated by ca. 13 cm^{-1}. The CCSD(T)/cc-pVTZ spectrum of **2a** predicts only two C−H stretching vibrations, separated by 20 cm^{-1}. The experimental spectrum of H−^{13}C−C−C−H (Figure 1) exhibits two C−H stretches differing by 16 cm^{-1}, in close agreement with the CCSD(T)/cc-pVTZ prediction. Another metric for differentiating the C_2 vs C_s structures involves the region near 1200 cm^{-1}. In this region, MP2/6-31G* predicts two IR vibrations of significant intensity, whereas CCSD(T)/cc-pVTZ predicts one vibration with zero intensity. Experiment agrees with the latter; no band is observed in this region. The experimental IR spectrum of H−C−^{13}C−C−H (from diazopropyne-2-^{13}C, **4b**) also exhibits good agreement with the computed spectrum for C_2-symmetric **2b** (CCSD(T)/cc-pVTZ). The accuracy of the coupled-cluster method in predicting the differential isotope shifts for the C−H and C−C stretching vibrations of the two isotopomers (−8 and −9 cm^{-1} for **2a**; 0 and −40 cm^{-1} for **2b**) engenders confidence in the prediction of a C_2-symmetric structure.

2. The ^{13}C-hyperfine splittings (hfs) in the experimental EPR spectra are consistent with a symmetrical structure (C_2) for triplet HCCCH and are inconsistent with an unsymmetrical structure (C_s). A matrix containing a single C_2-symmetric species (**2a**) would exhibit an EPR spectrum with only one set of hfs constants, while a matrix containing an equilibrium mixture of two C_s, acetylenic carbenes (**3a** and **3c**) would yield an EPR spectrum consisting of a superposition of two spectra with two different sets of hfs constants. (Localized structures **3a** and **3c** may be expected to exhibit different ^{13}C-hfs constants because of differing hybridization and spin densities at the nonequivalent terminal carbons.) Satisfactory simulation of the experimental spectrum of triplet HCCCH in the X_2 and Y_2 region was obtained with a single set of hyperfine splitting constants, $A_X = A_Y =$ 38 G (Figure 4). Attempted simulations of a 1:1 mixture of species with two different hfs constants, of plausible magnitude, resulted in poor fits to the experimental spectrum. Although the latter represents negative evidence against the localized carbenes **3a** and **3c**, we take the excellent fits for the spectral simulations of **2a** ($A_X = 38$ G) and **2b** ($A_X = 24$ G) (Figure 4), along with the photoequilibrated mixture of **2a** and **2b** (Figure 5), as solid evidence for a C_2 structure for triplet HCCCH.

3. Experimentally determined values for the ^{13}C-isotropic hyperfine splitting constants, A_I (C-1) = 28 G, A_I (C-2) = 19 G (Table 2), exhibit excellent agreement with the isotropic Fermi contact coupling constants predicted for the C_2-symmetric species (**2**), A_I (C-1) = 26.6 G, A_I (C-2) = −19.7 G (Table 3). The experimental values are inconsistent with those predicted for structure **1** or **3** (Table 3).

4. Estimated HCC and CCC bond angles, obtained from analysis of triplet EPR data (163° and 172°, respectively; *vide infra*) exhibit good agreement with those predicted for the C_2-symmetric species (**2**) (162° and 175°, respectively; Table 3).

All contemporary computational studies agree that the triplet potential energy surface for HCCCH structures **1**−**3** is very flat.[17,32−38] Barriers to interconversion lie below the zero-point vibrational energy. This situation defines triplet HCCCH as a quasilinear molecule. The molecular spectroscopy of quasilinear molecules has been considered in detail.[53−57] Two close analogues of triplet HCCCH—triplet cyanocarbene (HCCN) and triplet iso-cyanocarbene (HCNC)—are quasilinear.[58] Dynamical processes in quasilinear molecules often include manifestations of tunneling and equilibrium isotope effects. Lingering difficulties in modeling the low-frequency IR bending vibration of triplet HCCCH, along with the existence of extensive vibronic coupling in the electronic absorption spectrum, reveal the extent to which triplet HCCCH poses a significant challenge to theory. Further study will be required to assess whether triplet HCCCH is a molecule for which the Born−Oppenheimer approximation breaks down, akin to NO_3.[59] The spectroscopic evidence available at the current time, namely low-resolution IR, UV/vis, EPR spectra (including the effects of isotopic substitution), is straightforwardly interpreted in terms of a C_2-symmetric structure (**2**).

Zero-Field Splitting (ZFS) Parameters *D* and *E* of Triplet HCCCH. The zero-field splitting parameters of triplet HCCCH isotopomers display a subtle dependence on matrix material (Table 1). The largest *D* values for **2** and **2a** are in nitrogen matrices, and the smallest are in argon. A similar dependence was observed for methylene (CH_2) in neon, argon, and krypton matrices;[60] for CCO in neon, argon, krypton, and xenon;[48] and for C_4 in neon and argon.[61] This effect has been ascribed to the influence of spin-orbit mixing of the triplet ground state with low-lying singlet states.[48,60,61] Spin-orbit mixing, mediated by an external heavy atom, increases with increasing atomic number of the external atom. Increased mixing of triplet and singlet states decreases the dipolar coupling in the triplet, thereby

(53) *Structures and Conformations of Non-Rigid Molecules*; Laane, J., Dakkouri, M., van der Veken, B., Oberhammer, H., Eds.; Kluwer: Dordrecht, 1993.
(54) Bunker, P. R. *Annu. Rev. Phys. Chem.* **1983**, *34*, 59–75.
(55) Winnewisser, B. P. In *Molecular Spectroscopy: Modern Research*; Rao, K. N., Ed.; Academic Press: Orlando, FL, 1985; Vol. III, pp 321−419.
(56) Winnewisser, M.; Winnewisser, B. P.; Medvedev, I. R.; De Lucia, F. C.; Ross, S. C.; Bates, L. M. *J. Mol. Struct.* **2006**, *798*, 1–26.
(57) Child, M. S. *Adv. Chem. Phys.* **2007**, *136*, 39–94.
(58) Nimlos, M. R.; Davico, G.; Giese, C. M.; Wenthold, P. G.; Lineberger, W. C.; Blanksby, S. J.; Hadad, C. M.; Petersson, G. A.; Ellison, G. B. *J. Chem. Phys.* **2002**, *117*, 4323–4339.
(59) Stanton, J. F. *J. Chem. Phys.* **2007**, *126*, 134309.
(60) Bicknell, B. R.; Graham, W. R. M.; Weltner, W., Jr. *J. Chem. Phys.* **1976**, *64*, 3319–3324.
(61) Graham, W. R. M.; Dismuke, K. I.; Weltner, W., Jr. *Astrophys. J.* **1976**, *204*, 301–310.

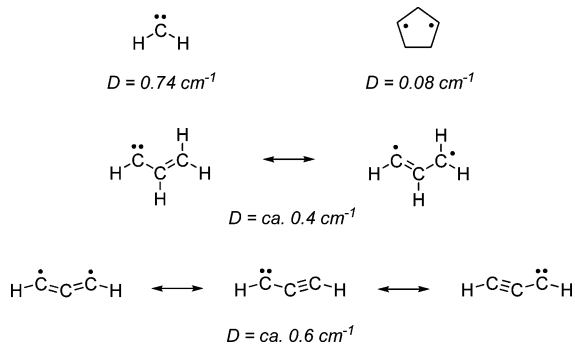

Figure 7. Experimental zero-field splitting parameter D for triplet carbenes and diradicals.

decreasing the D value. Our experimental determination of slightly smaller D values in argon, vs. nitrogen or methane, is consistent with this interpretation.

Comparison of the zfs parameter D of HCCCH with those of other small triplet molecules reveals another interesting trend. The D values increase in the series HCCCH ($|D/hc| = 0.6401$ cm^{-1}, in argon), CCO ($|D/hc| = 0.7107$ cm^{-1}, in argon),[48,63] HCCN ($|D/hc| = 0.8629$ cm^{-1}, in poly(chlorotrifluoroethylene)),[23] CNN ($|D/hc| = 1.145$ cm^{-1}, in argon),[48] and NCN ($|D/hc| = 1.544$ cm^{-1}, in perfluorinated glasses).[62] Each of these triplets has 14 valence electrons and a π-system for which important resonance contributors may have either allenic diradical or acetylenic carbene character. The D values increase as heteroatoms (N or O) are introduced into the molecules. Qualitatively, the unpaired electrons are drawn to the electronegative heteroatom(s), causing a stronger interaction that is reflected in a larger D value.

The interpretation of the large D value for triplet propynylidene has been problematic within the carbene chemistry community.[64] In light of our current investigation, as well as recent, related studies of dialkynyl carbenes,[65,66] it is important to offer a critical assessment of this issue. The dominant contribution to D involves dipolar coupling of the unpaired spins.[67,68] The magnitude of this coupling is inversely related to the distance between the two spins. Limiting cases are illustrated by methylene and cyclopentane-1,3-diyl (Figure 7). The unpaired spins in methylene are localized on the same atom, and their strong dipolar coupling leads to a large D value (0.74 cm^{-1}).[69,70] Conversely, the unpaired spins in cyclopentane-1,3-diyl experience a much larger average separation, leading to a much weaker dipolar coupling and a smaller D value (0.08 cm^{-1}).[71]

Many triplet carbenes possess an electronic structure in which a singly occupied orbital of σ-symmetry is localized at the carbene carbon, while a singly occupied orbital of π-symmetry is delocalized across the carbene substituent(s). As illustrated by the example of vinyl carbene, the delocalization of the π-electron gives a larger average separation of the unpaired spins, relative to methylene, leading to a smaller D value (0.4 cm^{-1}).[39,72] It is precisely in this context that the D value of triplet propynylidene (0.6 cm^{-1}) seems anomalously large. Indeed, the large D value has been taken as (i) evidence for a bent, localized carbene structure (**3**, C_s) that does not differ substantially in structure from triplet vinyl carbene and (ii) evidence against a 1,3-diradical structure.

The qualitative expectation that triplet propynylidene exhibits a greater degree of electronic delocalization than triplet vinyl carbene is accurate. The expectation that this greater delocalization manifests itself in terms of a smaller D value, however, is not. Unlike triplet vinyl carbene, triplet propynylidene does not possess a singly occupied orbital of σ-symmetry that is localized at the carbene carbon. Rather, acetylenic carbenes consist of two orthogonal singly occupied orbitals of π-symmetry that are delocalized across the carbene substituent(s). In his seminal analysis of the zero-field splitting parameters of acetylenic carbenes, Wasserman recognized that, because both unpaired spins are delocalized, the one-center dipolar couplings are maintained not only at C-1 but also at C-2 and C-3.[64] That the one-center couplings are maintained at C-1 and C-3 is readily understood through consideration of hyperfine coupling constants (Table 2), spin densities (Table 4), and resonance structures (*vide infra*). The involvement of a one-center contribution at C-2, however, is not obvious from consideration of resonance structures. This contribution to the dipolar coupling occurs as a consequence of spin polarization and the accrual of negative spin density at C-2 (Table 4). One of the important findings from the current investigation is the experimental verification of substantial negative spin density at C-2 through the measurement of the ^{13}C hyperfine coupling constant.

The picture that emerges from the current study is fully consistent with Wasserman's earlier analysis. Indeed, substituting our computed spin densities (Table 4) into his analysis yields a predicted D value for triplet propynylidene of 0.6 cm^{-1}, a value in surprisingly good agreement with the experimental value. As Wasserman established in his original study, the one-center contribution arising from spin polarization at C-2 represents an important contribution to D; neglecting this term affords a predicted D value of 0.33 cm^{-1}.[64] The reason that our analysis yields a larger D value than the original investigation is a direct result of the fact that our calculations predict greater negative spin density at C-2.

To restate our findings, succinctly, the large D value of triplet propynylidene arises from one-center dipolar couplings of the unpaired spins at each position along the carbon chain. The large magnitude of D is neither evidence in support of a bent, localized carbene structure nor evidence against a 1,3-diradical structure.

Bernheim, Skell, and co-workers reported $E = 0.0000 \pm 0.0008$ cm^{-1} for triplet HCCCH in poly(chlorotrifluoroethylene) at 77 K and interpreted this result in terms of a linear structure

(63) DeKock, R. L.; Grev, R. S.; Schaefer, H. F., III. *J. Chem. Phys.* **1988**, *89*, 3016–3027.
(62) Wasserman, E.; Barash, L.; Yager, W. A. *J. Am. Chem. Soc.* **1965**, *87*, 2075–2076.
(64) Wasserman, E. *J. Chem. Phys.* **1965**, *42*, 3739–3740.
(65) Bowling, N. P.; Halter, R. J.; Hodges, J. A.; Seburg, R. A.; Thomas, P. S.; Simmons, C. S.; Stanton, J. F.; McMahon, R. J. *J. Am. Chem. Soc.* **2006**, *128*, 3291–3302.
(66) Thomas, P. S.; Bowling, N. P.; McMahon, R. J. *J. Am. Chem. Soc.* **2009**, in press.
(67) Wertz, J. E.; Bolton, J. R. *Electron Spin Resonance Spectroscopy*; Chapman and Hall: New York, 1986.
(68) Weltner, W., Jr. *Magnetic Atoms and Molecules*; Van Nostrand Reinhold: New York, 1983.
(69) Wasserman, E.; Yager, W. A.; Kuck, V. J. *Chem. Phys. Lett.* **1970**, *7*, 409–413.
(70) Wasserman, E.; Kuck, V. J.; Hutton, R. S.; Yager, W. A. *J. Am. Chem. Soc.* **1970**, *92*, 7491–7493.
(71) Dougherty, D. A. In *Kinetics and Spectroscopy of Carbenes and Biradicals*; Platz, M. S., Ed.; Plenum Press: New York, 1990, pp 117–142.
(72) Hutton, R. S.; Manion, M. L.; Roth, H. D.; Wasserman, E. *J. Am. Chem. Soc.* **1974**, *96*, 4680–4682.

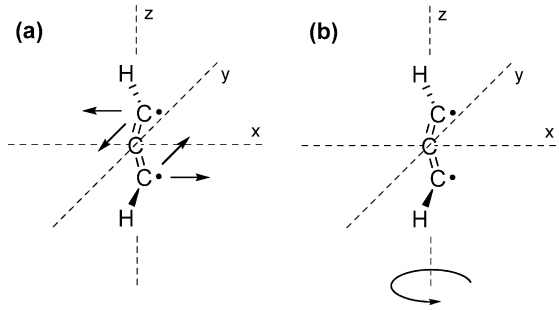

Figure 8. (a) Partial rotation of the long axis of propynylidene (**2**) about either the *x*- or *y*-molecular axis, constituting a precession or a wobble. This motion decreases the zero-field splitting parameter *D*. (b) Rotation of propynylidene (**2**) about the *z*-molecular axis (the long axis of the molecule). This motion is relatively unhindered and causes a substantial decrease in the zero-field splitting parameter *E* by inducing effective cylindrical symmetry.

1.[23] (A molecule with a 3-fold axis of symmetry, or higher, must exhibit $E = 0$.[67,68]) Our EPR experiments in both argon and nitrogen at 15 K afford somewhat higher resolution, which enabled us to detect structure in the XY_2 transition and therefore measure small, but nonzero, values of *E* for the isotopomers of triplet HCCCH (Table 1). Our values of *E* fall roughly within the error limits reported by Bernheim et al.[23,73] Qualitatively, the very small measured *E* indicates a molecule of near axial symmetry. As we shall see in the following section, however, the interpretation of *D* and *E* is further complicated by motional effects in the matrix.

Motional Effects on ZFS Parameters *D* and *E*. The zfs parameters are subject to motional averaging; both *D* and *E* decrease as motion increases. The effects of motional averaging on the zfs parameters of methylene (CH_2) have been extensively investigated,[48,69,70,74,75] and we will consider our EPR data for propynylidene in light of the theoretical treatment employed in those studies.

The small, but real, disparity in the *D* values measured for unlabeled propynylidene (**2**) and propynylidene-*d* (**2d**) in argon provide evidence for zero-point motion in the matrix sites. The motion affecting *D* is a type of precession or wobble, described by a partial rotation of the long axis (*z*-axis) of the molecule about the *x*- and *y*-molecular axes (Figure 8a). This type of motion in matrices has been established for CH_2,[69,70,75] CCO and CNN,[48] and O_2.[76,77] If one assumes that this motion occurs in a restrictive potential well of the form

$$V = V_o(1 - \cos 2\varphi) \tag{1}$$

where φ is the angle of oscillation of the *z*-axis from its equilibrium position and V_o is the potential maximum, then one may derive the following relationship, assuming the harmonic oscillator approximation is valid for the motion.[77]

$$D = D_m\left[1 - ({}^3/_4)(\hbar^2/IV_o)^{1/2}\right] \tag{2}$$

D is the observed zero-field splitting parameter, D_m is the zfs parameter of the molecule rigidly fixed by the matrix, and *I* is the moment of inertia of the molecule. D_m is equivalent to the gas-phase *D* if the molecule is unperturbed by the matrix. Assuming that V_o is the same for two isotopomers, then the deviation of *D* from its fixed value for the two species is

$$(D_m - D_1)/(D_m - D_2) = (I_2/I_1)^{1/2} \tag{3}$$

Obtaining *I* by independent means, one may calculate D_m from the measured *D* values of the two isotopomers **2** and **2d**. The moments of inertia *I* for **2** and **2d** are not known experimentally; however, they may be estimated from the computed rotational constants (Table S3). Approximating propynylidene as a symmetric rotor, then $I_{||}$ is related to the rotational constant *A* by

$$I_{||} = \hbar^2/2A \tag{4}$$

Using the computed *A* of 3105.7 GHz for **2** and 2367.4 GHz for **2d**, the moments of inertia $I_{||}$ are 2.70×10^{-48} and 3.54×10^{-48} kg m^2, respectively. From eq 3, D_m for propynylidene is 0.6779 cm^{-1} (in argon), 5.9% greater than the observed *D* of **2**. Insertion of this D_m into eq 2 yields $V_o = 18\,400$ cm^{-1} as the barrier to oscillation for **2**. This barrier is very large compared to those of CH_2 (122 cm^{-1}, in xenon),[69,70,75] CCO (240 cm^{-1}, in neon),[48] and O_2 (152 cm^{-1}, in nitrogen).[77] Propynylidene is about twice as long as each of these and thus would sweep out a much larger arc upon full rotation about the *x*- or *y*-molecular axis. The solid argon matrix would constrain this motion to a much greater extent for **2** than for the aforementioned smaller molecules, thus making the large calculated barrier reasonable. The ^{13}C-isotopomers **2a** and **2b** exhibit *D* larger than that for unlabeled **2**, consistent with the above analysis. Their moments of inertia *I*, however, are only slightly larger than that of **2**, because the isotopic substitution is much closer to the molecular center of mass than in **2d**. Thus, the differences in *D* for **2a** and **2b** relative to **2** are much smaller than that for **2d** (Table 1).

A second interpretation of the differing *D* for isotopomers of propynylidene is possible: variation in *D* arising from subtle changes in bond lengths upon isotopic substitution.[48] Since *D* is proportional to $\langle 1/r^3 \rangle$ (where *r* is the distance between the two unpaired electrons), a 0.1% decrease in bond length results in a 0.3% increase in *D*. Deuterium substitution decreases C−H(D) bond lengths by 0.002 to 0.003 Å,[78] ca. 0.2 to 0.3%, which could result in a 0.9% increase in *D* (upper limit). The *D* value of DCCCH (**2d**) is 0.7% greater than that of HCCCH (**2**), which is approximately the difference one would expect for the corresponding decrease in C−H(D) bond length. The validity of this interpretation, however, requires an unrealistically large spin density (near unity) on the hydrogen atoms. The computed NBO spin density on H in propynylidene is only −0.04 (Table 3). Thus, we consider bond length effects as a negligible factor affecting *D* in propynylidene, and we interpret the change in *D* upon isotopic substitution as evidence of oscillatory motion of propynylidene in the matrix.

The motion that affects *E*, in a triplet molecule, is rotation about the *z*-molecular axis (Figure 8b). Following the methylene case, if one assumes that propynylidene is a free rigid rotor in a plane, with rotational energy levels $W_J = BJ^2$ and moving in a potential well of the form shown in eq 1, then the rotational

(73) Bernheim, R. A.; Kempf, R. J.; Reichenbecher, E. F. *J. Magn. Reson.* **1970**, *3*, 5–9.
(74) Bernheim, R. A.; Adl, T.; Bernard, H. W.; Songco, A.; Wang, P. S.; Wang, R.; Wood, L. S.; Skell, P. S. *J. Chem. Phys.* **1976**, *64*, 2747–2755.
(75) Wasserman, E.; Hutton, R. S. *Acc. Chem. Res.* **1977**, *10*, 27–32.
(76) Meyer, H.; O'Brien, M. C. M.; Van Vleck, J. H. *Proc. R. Soc. London, Ser. A* **1958**, *243*, 414–421.
(77) Kon, H. *J. Am. Chem. Soc.* **1973**, *95*, 1045–1049.
(78) Laurie, V. W.; Herschbach, D. R. *J. Chem. Phys.* **1962**, *37*, 1687–1693.

barrier will mix in the first rotational state of the appropriate symmetry (which is $J = 2$). Wasserman et al. derived eq 5 from this theoretical treatment, relating the observed E to that of a fixed rotor, E_m, by the ratio of the rotational barrier to the energy of the second rotational level.

$$E = E_m(V_2/W_2) \tag{5}$$

Neither V_2 nor W_2 was known for CH_2, but by expressing both V_2 and W_2 in terms of α (one-half the bond angle at the carbene carbon), E_m was obtainable. V_2 was related to α by eq 6,

$$V_2 = 122(^6/_7)^2 \cot^2 \alpha \ \ \mathrm{cm}^{-1} \tag{6}$$

The factor of $^6/_7$ derives from the z-molecular axis not passing through the C atom but lying ca. $^1/_7$ of the way out to the line which passes through both H atoms, reducing the hydrogen displacement on rotation by $^1/_7$. Most importantly, the following assumption was made: the barrier to rotation about the z-molecular axis (affecting E) takes the same form as rotation about the x- and y-molecular axes (affecting D, *vide supra*) and thus has the same barrier constant, $V_2 = 122\ \mathrm{cm}^{-1}$. This assumption most certainly does not hold for HCCCH, which is at least twice as long (in the z-direction) as CH_2 but is not as "wide" (in the $x-y$ plane) because of the larger bond angles. Thus, the barriers to rotation in the two directions should be quite different. Without knowing what the barrier for rotation about the z-axis might be, we are unable to calculate E_m. Nevertheless, the implication of a motional effect on D for HCCCH (**2**) strongly implicates a motional effect on E, as well, since the motion affecting E is expected to be much more facile.

If the influence of motional effects on zfs parameters is manifest in our experiments (Ar, N_2, CH_4; 15 K), then the influence of these effects would be even more pronounced under the conditions of Bernheim and Skell (poly(chlorotrifluoroethylene); 77 K). Indeed, their spectrum exhibits a single XY_2 transition with no hint of structure attributable to separate X_2 and Y_2 transitions.[23] The key point of difference between our study and the earlier study is the interpretation of the very small E value. Rather than concluding that the small E value arises from an axially symmetric structure (**1**),[23] we conclude that the E value is anomalously low because of the effect of motional averaging. The small E value is not necessarily a diagnostic signature of an axially symmetric structure.

Estimation of Bond Angles in Triplet HCCCH. The ratio E/D is occasionally used to estimate the bond angle at the divalent carbon in carbenes. The expression derived by Wasserman et al.[69,70,75] relating E_m/D_m to the carbene bond angle (2α) is

$$(E_m/D_m) = (\cos^2 \alpha)/(2 - 3\cos^2 \alpha) \tag{7}$$

It is not obvious, however, that this analysis is appropriate for a molecule such as triplet HCCCH (**2**). Additional discussion concerning this matter is provided in the Supporting Information.

A second, independent method for gaining structural information from EPR spectra derives from the isotropic ^{13}C-hyperfine splitting constant, A_I. The isotropic hyperfine interaction is unaffected by the motion of the molecule in the matrix site, unlike the zfs parameters D and E. The largest contribution to A_I is typically the Fermi contact splitting due to the interaction of the unpaired spin density at the ^{13}C nucleus with the magnetic nucleus itself. The Fermi contact term gives a direct measure of the s character of the orbital in which the unpaired spin resides; A_I is an increasing function of the percent s character of that orbital. The road from the measured hyperfine constants to the bond angles at the ^{13}C-labeled nuclei is rather lengthy and approximation-laden, and the estimated bond angles should be regarded accordingly. The complete analysis is available in the Supporting Information. To summarize the key findings, the terminal bond angle, a(HCC), *does* deviate from linearity. The experimentally derived bond angles for propynylidene (**2**) are $a(\mathrm{HCC}) = 163°$ and $a(\mathrm{CCC}) = 172°$. These values display good agreement with the computed (QCISD/6-311+G(2df,p)) bond angles of 162° and 175°, respectively.

Computational Population Analysis of Triplet HCCCH. The Natural Bond Orbital (NBO) analysis of triplet HCCCH (**2**) reveals that electron density migrates from the hydrogen atoms to the carbon atoms; C-2 accumulates the most negative charge (Table 4). Dividing the electron population into α- and β-spins is instructive. An excess of α-spin density accrues at C-1 and C-3 (beyond the expected population of 2.5 at these carbons) with a corresponding depletion of α-spin density at C-2 (Table 4). A surplus of β-spin density collects at C-2 (beyond the expected 2.0) at the expense of β-spin density at C-1 and C-3. Spin polarization of this sort is well-established in the literature of aromatic and other π-delocalized radicals[67] and has been considered in the context of aryl carbenes.[79] The magnitude of spin polarization of $\rho(\mathrm{C\text{-}1, C\text{-}3}) = 0.621$ and $\rho(\mathrm{C\text{-}2}) = -0.200$ (normalized to one) for **2** exceeds that in the analogous allyl radical, where $\rho(\mathrm{C\text{-}1, C\text{-}3}) = 0.582$ and $\rho(\mathrm{C\text{-}2}) = -0.164$.

The NBO analysis of the α-spins details the spin polarization (Table 5). The σ-bonds are unexceptional. The α-spin in the π-bonds is strongly polarized toward the terminal carbons, ~70%, and the occupancy is nearly unity. The nonbonded electrons are partitioned between NAOs of nearly pure p-orbital character at C-1 and C-3 (occupancy of 0.75) and the antibonding π-orbitals (occupancy of 0.23). The polarization in the π*-orbitals is 70% toward C-2. The population in the π*-orbitals indicates delocalization of the nonbonded α-spins and provides a mechanism for greater interaction between these electrons at C-2.

The NBO analysis of the β-spins is at first a bit puzzling. Again, the σ-bonds are not noteworthy. The π-NBOs are strongly polarized toward C-2, ca. 77%, and have a relatively low occupancy of 0.78. Both of the π-bonds, however, are located between C-1 and C-2. The remaining β-spin density is located at C-3 in NAOs of nearly pure p-orbital character. If the occupancy of the π-NBOs (0.78) is multiplied by the β-spin at C-1 in the π-bonds (23%) the result is 0.18, which is nearly equivalent to the β-spin of 0.20 at C-3. The small difference is made up by the β-spin in the π*-NBOs of C-1 and C-2. Thus, the β-spin is effectively symmetrical, as is the α-spin, but is substantially polarized to C-2.

A different approach to presenting the population analysis employs Natural Resonance Theory (NRT). NRT determines, from the NBO data, the valence bond representations (i.e., resonance structures) contributing to the wave function. The important resonance structures for triplet propynylidene (**2**) are presented in Figure 9. For the α-spins, a diradical-like structure constitutes 49% of the overall wave function; however, taken together, two carbenic structures contribute nearly the same amount, 46%. Twelve other Lewis structures are found, but each contributes <1% to the overall structure. Two are tris-carbenes; the other ten are "no bond" structures, with broken σ-bonds. The β-spins have three important resonance structures as well: one allenic and two acetylenic, with nearly the same percent contribution as the correspond-

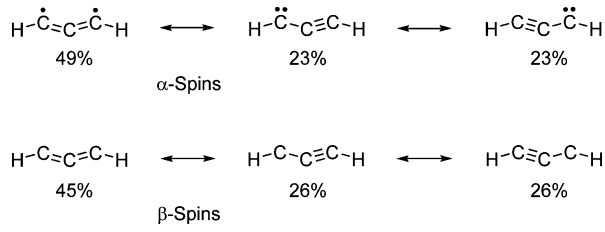

Figure 9. Natural Resonance Theory (NRT) description of triplet HCCCH.

ing α-spin structures. Together, the carbene-like resonance structures contribute 7% more than the diradical, which may explain why the NBO populations for the β-spins in Table 6 appear in terms of a triple bond (*vide supra*). Six other structures contribute <1%.

In a very simple way, the NRT analysis highlights an important concept: the electronic structure of triplet HCCCH may be best formulated as an admixture of diradical and carbene. This proposition helps explain the relatively large zfs parameter of $D = 0.6401$ cm^{-1} for **2**. This large D value requires a significant degree of interaction between the two unpaired electrons. The carbene resonance structures illustrate the mechanism for this enhanced one-center electronic interaction in **2**. The large degree of negative spin density on the central carbon of **2** may also increase the magnitude of D due to interactions within the accumulated β-spin. The significant α-spin density in the π*-NBOs at C-2 may contribute to a larger D, as well.

Summary

Spectroscopic investigations of mono-^{13}C and ^{2}H isotopomers of triplet HCCCH provide a body of data that is interpretable in terms of a C_2-symmetric, 1,3-allenic diradical structure (**2**). The molecule is quasilinear, with a barrier to linearity that lies below the zero-point vibrational energy. Experimental IR spectra and isotope shifts are in good accord with the predictions from ab initio calculations. EPR data, including zero-field splitting parameters and hyperfine coupling constants, are consistent with a C_2-symmetric structure **2**, after taking proper consideration of contributions from dipolar couplings and motional effects in matrices. Analysis of the hyperfine coupling constants affords an experimentally based estimate for the HCC bond angle of ca. 163°. Rather than attempting to categorize triplet HCCCH as a carbene vs a diradical, analysis in terms of Natural Resonance Theory suggests that triplet HCCCH is best viewed as an equal admixture of both.

Methods

Computational Methods. Ab initio calculations were performed at the QCISD level of theory,[80] with the 6-311+G(2df,p) basis set,[81] as implemented in *Gaussian03*.[82] Refined predictions for the isotropic Fermi contact couplings were obtained using the procedure of Barone (B3LYP/EPR-III).[52] Natural Bond Orbital (NBO) and Natural Resonance Theory (NRT) calculations were performed as implemented in the Gaussian suite of programs.[50]

Experimental Methods. The experimental technique and apparatus for low-temperature matrix-isolation spectroscopy have been described previously.[83,84] Infrared spectroscopy employed a Nicolet 740 FTIR instrument (liquid N_2 cooled MCT-B detector). Ultraviolet−visible spectroscopy was performed with a Hitachi U-3210 spectrometer. EPR experiments employed a Bruker ESP 300 E spectrometer at X-band with a Bruker ER 042 MRHE microwave bridge. An EIP microwave counter (model 625A CW) provided the microwave frequency. The EPR spectra of propynylidene (**2**) matrix-isolated in nitrogen were obtained employing a Varian E-15 X-band spectrometer with a Varian E-101 microwave bridge. The zero-field splitting parameters were calculated by the best fit of the EPR spectra with the spin Hamiltonian,[85] with the assumption that $g_x = g_y = g_z = g_e$. This assumption has been shown to be valid by Bernheim et al.[73]

Diazopropyne (4), Diazopropyne-1-^{13}C (4a), Diazopropyne-2-^{13}C (4b), Diazopropyne-3-^{13}C (4c), Diazopropyne-2-^{13}C (4c), and Diazopropyne-3-*d* (4d). Diazo compounds were prepared by pyrolysis of the corresponding tosylhydrazone salts. The syntheses of the ^{13}C-labeled tosylhydrazones are reported elsewhere.[86] *Caution! Alkynyl diazo compounds, including diazopropyne (**4**), are highly reactive and often explosive*. Synthesis and manipulation of these compounds require extreme caution. We encountered one explosion of **4**, and others have as well.[87] Appropriate safety precautions must be observed. We worked with small quantities (< 50 mg) of diazopropyne, keeping the sample cold (−94 °C) and under vacuum or dry nitrogen atmosphere to minimize the risk of explosion.

Freshly prepared tosylhydrazone salt was placed in a 10-mL round-bottom flask. A glass adapter arm (essentially a short-path distillation column) connected the flask to a collection tube. The system was evacuated (<1 Torr), and the salt was heated to 40 °C for 15 min. Pyrolysis was then effected by raising the temperature to 70 °C for 60 min. The yellow diazopropyne condensed in the collection tube, which had been cooled with liquid N_2. The liquid N_2 bath was replaced with a hexane slush bath (−94 °C), and the system was vented with dry N_2. After the collection tube was transferred to the matrix-isolation apparatus, the sample was subjected to two freeze−pump−thaw cycles at −94 °C. After the pressure in the matrix-isolation system had fallen below 5×10^{-6} Torr, diazopropyne was sublimed from the −94 °C slush bath and codeposited with argon on a cold window maintained at 30 K (for IR and UV/vis experiments) or codeposited with argon, nitrogen, or methane on a copper tip at 15 K (for EPR experiments). **4**: IR (Ar, 10 K) 3333 s, 3320 w, 3098 w, 2123 m, 2117 w, 2072 vs, 1362 w, 1353 w, 1054 m, 827 w, 700 w, 683 m, 616 w, 528 m, 475 m, 360 w, 355 w, 350 m cm^{-1}; **4a**: IR (Ar, 10 K) 3338 w, 3332 s, 3091 w, 2120 m, 2104 w, 2091 w, 2064 vs, 1364 w, 1328 m, 1052 m, 821 w, 700 w, 683 m, 615 w, 527 m, 470 m cm^{-1}; **4b**: IR (Ar, 10 K) 3332 m, 3098 w, 2110 s, 2096 s, 2052 vs, 1361 w, 1354 w, 1054 m, 685 w, 610 w, 528 m, 471m, 353 w, 344 m cm^{-1}; **4c**: IR (Ar, 10 K) 3317 s, 3305 w, 3097 w, 2115 w, 2108 m, 2065 vs, 1353 w, 1049 m, 824 w, 678 w, 614 vw, 525 m, 474 m cm^{-1}; **4d**: IR (Ar, 10 K) 3098 w, 2610 m, 2597 m, 2124 m, 2118 m, 2087 vs, 1351 w, 1068 w, 1053 w, 977 vw, 957 vw, 819 w, 814 w, 682 w, 534 w, 528 w, 476 m cm^{-1}.

(79) Brandon, R. W.; Closs, G. L.; Davoust, C. E.; Hutchison, C. A.; Kohler, B. E.; Silbey, R. *J. Chem. Phys.* **1965**, *43*, 2006–2016.
(80) Pople, J. A.; Head-Gordon, M.; Raghavachari, K. *J. Chem. Phys.* **1987**, *87*, 5968–5975.
(81) Frisch, M. J.; Pople, J. A.; Binkley, J. S. *J. Chem. Phys.* **1984**, *80*, 3265–3269.
(82) Frisch, M. J.; et al. Gaussian 03, revision C.01; Gaussian, Inc.: Wallingford, CT, 2004.
(83) Seburg, R. A.; McMahon, R. J. *J. Am. Chem. Soc.* **1992**, *114*, 7183–7189.
(84) McMahon, R. J.; Chapman, O. L.; Hayes, R. A.; Hess, T. C.; Krimmer, H.-P. *J. Am. Chem. Soc.* **1985**, *107*, 7597–7606.
(85) Wasserman, E.; Snyder, L. C.; Yager, W. A. *J. Chem. Phys.* **1964**, *41*, 1763–1772.
(86) Seburg, R. A.; Hodges, J. A.; McMahon, R. J. *Helv. Chim. Acta* **2009**, in press.
(87) Wierlacher, S.; Sander, W.; Marquardt, C.; Kraka, E.; Cremer, D. *Chem. Phys. Lett.* **1994**, *222*, 319–324.

Acknowledgment. We gratefully acknowledge the National Science Foundation for support of this research. R.A.S. thanks the National Science Foundation and the Lubrizol Corporation for graduate fellowships. We thank Dr. Jeffrey T. DePinto for EPR spectra of HC_3H in nitrogen matrices, Prof. John F. Stanton (Univ. Texas) for illuminating conversations, and the reviewers for their careful reading of the manuscript and helpful comments.

Supporting Information Available: Estimation of bond angles and *D* value in triplet HCCCH (**2**); EPR hyperfine simulations of triplet HCCCH (**2a**, **2b**); UV/vis spectra of triplet HCCCH (**2**, **2a**); experimental and computed IR spectra for triplet HCCCH (**2**, **2a**, **2d**); computed IR harmonic vibrational frequencies and intensities for triplet C_s-structures (**3a**, **3c**); Cartesian coordinates for computed structures; complete literature citation for ref 82. This material is available free of charge via the Internet at http://pubs.acs.org.

JA901606A